SPATIAL DISTRIBUTION REQUIREMENTS OF REFERENCE GROUND CONTROL FOR ESTIMATING LIDAR/INS BORESIGHT MISALIGNMENT

A. Pothou[a,*], C. Toth[c], S. Karamitsos[b], A. Georgopoulos[a]

[a] Laboratory of Photogrammetry - (apothou, drag)@central.ntua.gr
[b] Laboratory of Higher Geodesy - karamits@central.ntua.gr
School of Rural & Surveying Engineering, National Technical University of Athens, Greece

[c]Center for Mapping, The Ohio State University, Columbus, OH 43212 USA – toth@cfm.ohio-state.edu

The 6th International Symposium on Mobile Mapping Technology (MMT'09)

KEY WORDS: Boresight misalignment, GPS, INS, Direct Georeferencing, MMS, LiDAR, Collocation

ABSTRACT:

LiDAR (Light Detection and Ranging, also known as Airborne Laser Scanning – ALS) is a powerful technology for obtaining detailed and accurate terrain models as well as precise description of natural and man-made objects from airborne platforms, with excellent vertical accuracy. High performance integrated GPS/INS systems provide the necessary navigation information for the LiDAR data acquisition platform, and therefore, the proper calibration of the entire Mobile Mapping System (MMS) including individual and inter-sensor calibration, is essential to determine the accurate spatial relationship of the involved sensors. In particular, the spatial relationship between the INS body frame and the LiDAR body frame is of high importance as it could be the largest source of systematic errors in airborne MMS. The feasibility of using urban areas, especially buildings, for boresight misalignment is still investigated. In this research, regularly or randomly distributed, photogrammetrically restituted buildings are used as reference surfaces, to investigate the impact of the spatial distribution and the distance between the necessary 'building-positions' on boresight's misalignment parameter estimation. The data used for performance evaluation included LiDAR point clouds and aerial images captured in a test area in London, Ohio, USA. The city includes mainly residential houses and a few bigger buildings.

1. INTRODUCTION

LiDAR systems are complex multi-sensory systems including: GPS (Global Positioning System) and INS (Inertial Navigation System) navigation sensors, and the laser-scanning device. Most of the newer systems also include a medium format digital camera to provide conventional image coverage of the surveyed area. LiDAR is considered as a basic component of modern airborne and terrestrial Mobile Mapping Systems (MMS) (Shan and Toth, 2008). The proper calibration of this MMS, including individual and inter-sensor calibration, is a must to achieve the highest accuracy of the output data. In particular regarding the boresight misalignment, the spatial relationship between the INS and LiDAR body frames is of high importance, as it could be the largest source of systematic errors in airborne MMS, and thus, must be determined before the system can be effectively utilized (Burman, 2000). In most installations, the lever arms between LiDAR/GPS/INS sensors can be determined separately by independent means, with good accuracy. In sharp contrast, the determination of the boresight angles is only possible in-flight once the GPS/INS derived orientation becomes sufficiently accurate (Skaloud and Lichti, 2006).

Despite several years of progress, the boresight estimation between the LiDAR and INS sensors is still heavily researched. Since the time when Baltsavias (1999), presented an overview of basic relations and error formulas concerning airborne laser scanning, a lot of research efforts have been devoted to investigate the effect and the elimination of boresight misalignment errors (Burman, 2000; Toth and Csanyi, 2001; Schenk, 2001; Toth, 2002; Morin and El-Sheimy; 2002; Scaloud and Lichti, 2006; Pothou *et al.,* 2007;. Habib *et al.,* 2007; Scaloud and Schaer, 2007). For extended literature review about boresight misalignment between the LiDAR and INS sensors, see Pothou *et al.* (2007) and Pothou *et al.* (2008).

An algorithm for observing and subsequently determining the boresight misalignment of LiDAR/INS, using two different surfaces (point datasets) was introduced by Pothou *et al.* (2007). The method minimizes the distances between points of the target surface and surface patches (TINs) of the reference surface, along the corresponding surface normals (based on Schenk *et al.,* 2000). The technique can be applied to various data combinations, such as matching LiDAR strips or comparing LiDAR data to photogrammetrically derived surfaces. Objects of simple shapes, similar to man-made structures such as buildings, have been chosen and used for surface matching. The processing algorithm includes additional testing of the validity, accuracy, and precision of various statistical tests (QA/QC - Quality Assurance/Quality Control) for outlier detection in the positioning and attitude data.

As a continuation research, Pothou *et al.* (2008) investigated the feasibility of using urban areas for boresight misalignment focusing on what the impact of the building shape, size, distribution, etc. is on the performance of the boresight misalignment process. Photogrammetrically restituted buildings were used as reference surfaces called 'building-positions', 'reference-positions' or simply 'positions'. The influence of the number and distribution of the necessary 'building-positions' on boresight's misalignment parameter estimation has been evaluated. Experiments with various number of 'building-positions' in regular as well as random distribution are presented, analyzed and evaluated through QA/QC statistical tests. The optimum number and distribution of 'building-positions' have been determined and proposed.

In this research, the impact of the spatial distribution and distance between the necessary 'building-positions' on boresight's

* Corresponding author

misalignment parameter estimation is evaluated by a collocation method. In Section 2, a short review of the status of multisensor calibration and boresight misalignment of LiDAR/INS is provided. The performance of the algorithm for determining boresight misalignment of LiDAR/INS is described in Section 3. Section 4 outlines the mathematical model of the algorithm which is based on a collocation adjustment method, and by which the minimum satisfying density of known 'reference positions' in the dataset for precise LiDAR/INS boresight misalignment parameters estimation, is calculated. In Section 5, the dataset used for testing is described. The processing, the experimental results as well as their statistical analysis and their effects on LiDAR points, are described in Section 6. Section 7 concludes the research.

2. MULTI SENSOR CALIBRATION - BORESIGHT MISALIGNMENT

The navigation solution is generally computed in the INS frame, usually considered as the local reference system of the MMS system. The spatial relationship between the laser scanner and the INS is defined by the offset and rotation between the two systems. To obtain the local object coordinates of a LiDAR point, the laser range vector has to be reduced to the INS system by applying the offset and rotation between the two systems, which provides the coordinates of the LiDAR point in the INS system. The mapping frame coordinates can be subsequently derived by the GPS/INS supported navigation solution. In our discussion, the determination of boresight values between the INS and the laser frame is addressed (Figure 1). Note that the offset components are frequently determined separately from the misalignment angles, using different technologies.

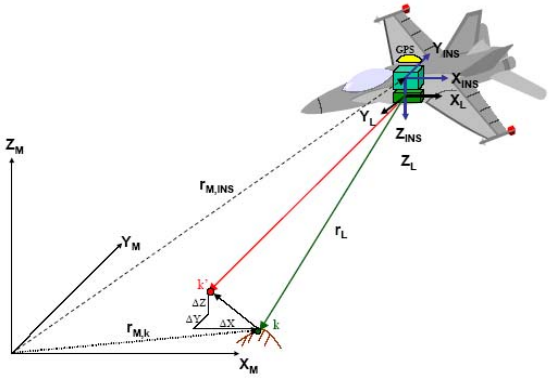

Figure 1. LiDAR system components

Assuming a highly accurate georeferencing solution, any discrepancy in boresight values results in a misfit between the LiDAR points and the ground surface, and thus, the calculated coordinates of the LiDAR points are not correct (Toth, 2002). Ideally, the calibration parameters should stay constant for subsequent missions. The description of the effects of the different boresight misalignment angles is omitted here; for details see (Baltsavias, 1999; Csanyi, 2008). For a detailed description of multisensor calibration – boresight misalignment, see Toth and Csanyi, 2001; Toth, 2002; Pothou *et al.,* 2007; Pothou *et al.,* 2008; and Csanyi, 2008.

3. AN ALGORITHM FOR DETERMINING BORESIGHT MISALIGNMENT

Two datasets, called point clouds P (x_{pi}, y_{pi}, z_{pi}) (p_i= 1,…, n) and Q (x_{qi}, y_{qi}, z_{qi}) (q_i= 1,…, m), which describe the same object(s) and are captured by different technologies, must be transformed into a common system. Assuming that these datasets are connected by a 6-parameter 3D transformation, the three offset and three rotation parameters can be estimated, minimizing the distance between a point of Q dataset and a TIN surface patch of P surface, which is described by points of P dataset (Equation [1]). In Figure 2, point q_i (x_{qi}, y_{qi}, z_{qi}) of Q point cloud has to be transformed to the closest surface patch of the control surface P, defined by 3 points (p_m, p_k, p_ℓ), through its projection q_i' (x_{qi}', y_{qi}', z_{qi}') onto the surface patch. The details for the algorithm were presented in Pothou *et al.,* 2006, (called algorithm B). Also in Pothou *et al.,* 2007 and Pothou *et al.,* 2008, analysis and performance evaluation of the boresight parameters estimation algorithm was discussed.
In Equation [1], **R** (ω, φ, κ) is the orthogonal rotation matrix, while b_x, b_y, b_z are the elements of the offset vector.

$$\begin{bmatrix} x_p \\ y_p \\ z_p \end{bmatrix} = \mathbf{R} \cdot \begin{bmatrix} x_q \\ y_q \\ z_q \end{bmatrix} + \begin{bmatrix} b_x \\ b_y \\ b_z \end{bmatrix} \quad (1)$$

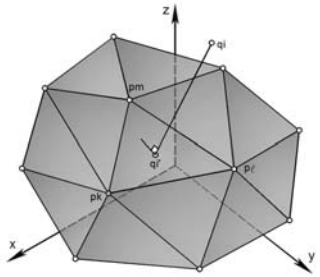

Figure 2: Transformation between q_i points and control surface P

In our approach, a TINs mesh for each building, by photogrammetrically derived points (p_m, p_k, p_ℓ), is constructed. The coordinates of q_i' (x_{qi}', y_{qi}', z_{qi}'), which correspond to projection of point q_i (x_{qi}, y_{qi}, z_{qi}) on the plane (p_m, p_k, p_ℓ), can be calculated as described by Pothou *et al.,* 2006. Equation [2] is the observation equation for each point in Q. After performing a Least Squares estimation, the solution of Equation [3] and the best estimation of the vector $\hat{\mathbf{x}}$ $\left(\hat{\omega}, \hat{\varphi}, \hat{\kappa}, \hat{b}_x, \hat{b}_y, \hat{b}_z\right)$, is provided by Equation [4]. **W** is a diagonal weight matrix of the observations, $\mathbf{x}^o$ is the vector of the approximated parameters and $\boldsymbol{\delta}\ell$ is the second part of the observation equation (Equation [3]). Matrices **T** and **L**, depend on the plane's parameters and **v** is the residual vector (for details see Pothou *et al.,* 2008).

$$(\mathbf{T} - \mathbf{I}) \cdot \left(\mathbf{R} \cdot \begin{bmatrix} x_{qi} \\ y_{qi} \\ z_{qi} \end{bmatrix} + \begin{bmatrix} b_x \\ b_y \\ b_z \end{bmatrix} \right) + \mathbf{L} = \mathbf{0} \quad (2)$$

$$\mathbf{A}\delta\mathbf{x} = \boldsymbol{\delta}\ell + \mathbf{v} \quad (3)$$

$$\hat{\mathbf{x}} = \mathbf{x}^o + \left(\mathbf{A}^T\mathbf{W}\mathbf{A}\right)^{-1}\mathbf{A}^T\mathbf{W}\boldsymbol{\delta}\ell \quad (4)$$

The covariance matrix $\hat{\mathbf{V}}_{\hat{x}}$ and the a posteriori variance $\hat{\sigma}_o^2$ are calculated in Equations [5] and [6], where r is the degree of freedom.

$$\hat{\mathbf{V}}_{\hat{x}} = \hat{\sigma}_o^2 \left(\mathbf{A}^T \mathbf{W} \mathbf{A}\right)^{-1} \quad (5)$$

$$\hat{\sigma}_o^2 = \frac{\mathbf{v}^T \mathbf{W} \mathbf{v}}{r} \quad (6)$$

Applying this algorithm for each building, which has been photogrammetrically restituted (P surface), in combination with available LiDAR strips (Q surface), a number of independent estimations of transformation parameters are provided.

In this research, the spatial distribution and distance between the necessary 'building-positions' on boresight's misalignment parameter estimation, is evaluated by collocation method.

The objectives of this research are the followings: (1) the introduction of a methodology for determining the maximum distance that could separate 'buildings positions' for determining the boresight misalignment parameters, and (2) the generation of a methodology for assessing the value of the deviation of the boresight misalignment parameters at any point in the surveyed area.

4. THE MATHEMATICAL MODEL OF COLLOCATION

The collocation method is a modification of the classical Least Squared adjustment fitting of a set of known values (Mikhail, 1976; Moritz, 1989; Cross, 1990). The collocation algorithm takes into account the possibility of the existence of a field, which is considered to affect the above values by a signal **s(x,y)**. This signal affects the adjustment function in all known or measured values as well as the prediction or interpolation which could be achieved in positions outside of the known values.

Signal **s** in most cases is unknown. It is assumed that it has a known variation, an initial estimation of which can be derived from the calculated covariance of the total known values. The whole issue of collocation adjustment is based on the determination of the covariance matrix $\mathbf{V_s}$ of signal **s**, of the positions with known values and also of those for which it is desirable to make a prediction or interpolation. This matrix is taken into account in the whole adjustment, as an addition to the traditional covariance matrix of observations $\mathbf{V}_\ell$ and therefore it has to be known or estimated.

The estimation of $\mathbf{V_s}$ is based on covariance functions obtained by adjustment of covariances which are calculated by the measured values of the available data. The most common procedure for the calculation of the covariance, is called "the stepping covariances' increasing". According to this approach, the covariance is provided as the average of (i, j) pairs of known-measured values ℓ_i, ℓ_j, which corresponds to known positions x_i, y_i and x_j, y_j. The distances r_{ij} between these known positions are within the selected increasing step d. In Equation [7], N_k is the number of values ℓ that are inside of the distance r_{ij}, n_k is the number of pairs (ℓ_i, ℓ_j) inside of r_{ij} and *k* is a counter of calculated covariance values.

$$C_k = \frac{1}{n_k} \sum_{1}^{n_k} \ell_i \ell_j \qquad 1 \le i, j \le N_k \quad (7)$$

Based on values C_k calculated from Equation [7] and the corresponding intervals, after adjustment the covariance function is provided, by which the value of covariance for any distance r_{ij} can be estimated and therefore the matrix $\mathbf{V_s}$ can be obtained. In the case of the collocation, the classical linearized least squared system, is given by Equation [8], in which the design matrix **A** depends on the chosen model to describe the connection between the physical quantities. This system is solved by Equation [9], and the best parameter values are given by Equation [10].

$$\mathbf{A}\,\boldsymbol{\delta}\hat{\mathbf{x}} = \boldsymbol{\delta}\ell + \boldsymbol{\delta}\hat{\mathbf{s}} + \hat{\mathbf{v}} \quad (8)$$

$$\boldsymbol{\delta}\hat{\mathbf{x}} = \left(\mathbf{A}^T \left(\mathbf{V}_\ell + \mathbf{V_s}\right)^{-1} \mathbf{A}\right)^{-1} \mathbf{A}^T \left(\mathbf{V}_\ell + \mathbf{V_s}\right)^{-1} \boldsymbol{\delta}\ell \quad (9)$$

$$\hat{\mathbf{x}} = \mathbf{x}^o + \boldsymbol{\delta}\hat{\mathbf{x}} \quad (10)$$

In the model of Equation [8], it is assumed that apart from the classical Gauss-Markov model about the properties of the measurements and the residuals, the expected value of signal **s** is zero, there is no correlation with measurements ℓ_i and its approximation value is taken as $\mathbf{s}^o$=**0,** (Equation [11]).

$$E\{\mathbf{v}\} = \mathbf{0} \quad E\{\mathbf{s}\} = \mathbf{0} \quad \mathbf{V}_{\mathbf{s}\ell} = \mathbf{0} \quad \mathbf{s}^o = \mathbf{0} \quad (11)$$

In Equations [8] and [9], as observations ℓ of the collocation mathematical model, the corresponding parameters of the $\hat{\mathbf{x}}$ of Equation [4] are used, and in matrix $\mathbf{V}_\ell$ the corresponding $\hat{\mathbf{V}}_{\hat{x}}$ solutions of each building are utilized.

The a posteriori variance of unit weight $\hat{\sigma}_o^2$ and the a posteriori covariance matrix of $\hat{\mathbf{x}}$ are calculated by Equations [14] and [15], based on $\hat{\mathbf{v}}$ and $\boldsymbol{\delta}\hat{\mathbf{s}}$ (signal's residuals), which are calculated by Equations [12] and [13].

$$\hat{\mathbf{v}} = \mathbf{V}_\ell^{-1} \left(\mathbf{V}_\ell + \mathbf{V_s}\right)^{-1} \left(\mathbf{A}\,\boldsymbol{\delta}\hat{\mathbf{x}} - \boldsymbol{\delta}\ell\right) \quad (12)$$

$$\boldsymbol{\delta}\hat{\mathbf{s}} = \mathbf{V_s}^{-1} \left(\mathbf{V}_\ell + \mathbf{V_s}\right)^{-1} \left(\mathbf{A}\,\boldsymbol{\delta}\hat{\mathbf{x}} - \boldsymbol{\delta}\ell\right) \quad (13)$$

$$\hat{\sigma}_o^2 = \frac{\boldsymbol{\delta}\hat{\mathbf{s}}^T \mathbf{V_s}^{-1} \boldsymbol{\delta}\hat{\mathbf{s}} + \hat{\mathbf{v}}^T \mathbf{V}_\ell^{-1} \hat{\mathbf{v}}}{n - m} \quad (14)$$

$$\hat{\mathbf{V}}_{\hat{x}} = \hat{\sigma}_o^2 \left(\mathbf{A}^T \left(\mathbf{V}_\ell + \mathbf{V_s}\right)^{-1} \mathbf{A}\right)^{-1} \quad (15)$$

The signal values' estimation in different positions from the measurements, are based on Equation [16], with a posteriori covariance matrix given by Equation [17]. In these equations, $\mathbf{V}_{\mathbf{s},\mathbf{s}_1}$ is the covariance matrix between the positions of the available measurements and the positions of the estimates, and $\mathbf{V}_{\mathbf{s}_1,\mathbf{s}_1}$ is the corresponding matrix only for the new positions. These matrices are calculated by the covariance function using the corresponding distances of positions.

$$\boldsymbol{\delta}\hat{\mathbf{s}}_1 = \mathbf{V}_{\mathbf{s},\mathbf{s}_1}^{-1} \left(\mathbf{V}_\ell + \mathbf{V_s}\right)^{-1} \left(\mathbf{A}\,\boldsymbol{\delta}\hat{\mathbf{x}} - \boldsymbol{\delta}\ell\right) \quad (16)$$

$$\hat{\mathbf{V}}_{\hat{\mathbf{s}}_1,\hat{\mathbf{s}}_1} = \hat{\sigma}_o^2 \mathbf{V}_{\mathbf{s},\mathbf{s}_1} \left(\left(\mathbf{V}_\ell + \mathbf{V_s}\right)^{-1} \mathbf{V}_{\mathbf{s},\mathbf{s}_1}^T - \mathbf{V}_{\mathbf{s},\mathbf{s}_1} \left(\mathbf{V}_\ell + \mathbf{V_s}\right)^{-1} \left(\mathbf{A}^T \left(\mathbf{V}_\ell + \mathbf{V_s}\right)^{-1} \mathbf{A}\right)^{-1} \left(\mathbf{V}_\ell + \mathbf{V_s}\right)^{-1} \mathbf{V}_{\mathbf{s},\mathbf{s}_1}^T\right) \quad (17)$$

5. DATA DESCRIPTION

The dataset, used for testing, was provided by ODOT (Ohio Department of Transportation) and CFM (The Center for Map-

ping, OSU). In London, Madison County, Ohio, LiDAR point clouds and direct digital aerial images were collected in several missions over an urban test area.

The 55 mm focal length DSS digital camera, with 9μm pixel size, was laboratory calibrated prior to the flights. The test area was simultaneously surveyed by an Optech ALTM 30/70 LiDAR system of the ODOT. At FOV of 40°, 50 Hz scanner frequency and 70 kHz pulse rate, the point density was about 5-8 points/m^2. A set of 16 images with adequate coverage of the region, which contained survey control points, was selected for our investigations. The flight plan consisted of two parallel strips and two perpendicular strips of LiDAR data and a block of 4 aerial images strips over the same area, each containing 4 images, see Figure 3. For both sensors, an integrated GPS/INS system provided the georeferencing. In addition, traditional aerotriangulation was performed on aerial images using GCPs measured by geodetic means (0.1m STDV) providing the EO (Exterior Orientation). The bundle adjustment resulted in accuracies of 0.08 meters in the X, Y directions and 0.10 meters in the Z direction.

In the central part of the survey (also called "test field") some buildings, mainly medium sized, have been selected and photogrammetrically restituted (reference point dataset). These buildings are located in the overlapping area, show in Figure 3; in the image mosaic, the selected buildings are numbered, and are used as the reference dataset. The area which is occupied by the selected group of buildings is about 300,000 m^2 with a perimeter of 2250 m.

Figure 3: Highlighted (numbered) buildings distributed in the area and LiDAR strips' orientation

6. PROCESSING AND RESULTS

In Pothou *et al.,* 2008, 24 buildings were captured by both LiDAR and aerial images. In this research, the best estimates $\hat{\mathbf{x}}$ of the boresight misalignment parameters $\left(\hat{\omega},\ \hat{\varphi},\hat{\kappa},\hat{b}_x,\hat{b}_y,\hat{b}_z\right)$ and the corresponding covariance matrices $\hat{\mathbf{V}}_{\hat{x}}$ for each of the available 24 buildings are calculated. The calculation took into account all the available LiDAR strips for each building, according to the methodology described by (Pothou *et al.,* 2008). A small number of buildings were removed during the processing.

Thereafter, based on Equation [7], the covariance C_k for each boresight parameter is calculated using the available solutions. As step d, twice of the average size of the buildings is chosen which is in the range of 15-25m. The distances r_{ij} are calculated from the centers of gravity of each building.

The covariance is calculated only for the three boresight angles $\left(\hat{\omega},\ \hat{\varphi},\hat{\kappa}\right)$ since the offset boresight parameters $\left(\hat{b}_x,\hat{b}_y,\hat{b}_z\right)$ can not be determined with sufficient accuracy (Burman, 2002, Kremer, 2006, Pothou *et al.,* 2008).

Next, a suitable covariance function is selected. The process is based firstly on the success of the fitting and secondly on the fact that the produced covariance matrix should satisfy the properties of such a matrix. Several functions, including polynomial, exponential, logarithmic and wave form functions are used. In terms of fitting, the best results come from a second degree function: $C(r)=a\bullet r^2+b\bullet r+c$. Note that other functions gave relatively quite good results too. Figure 4 shows the fitted covariance curve C(r) to the calculated covariances C_k per counter k for the angle ω of the boresight; note that φ has similar behaviour with ω angle.

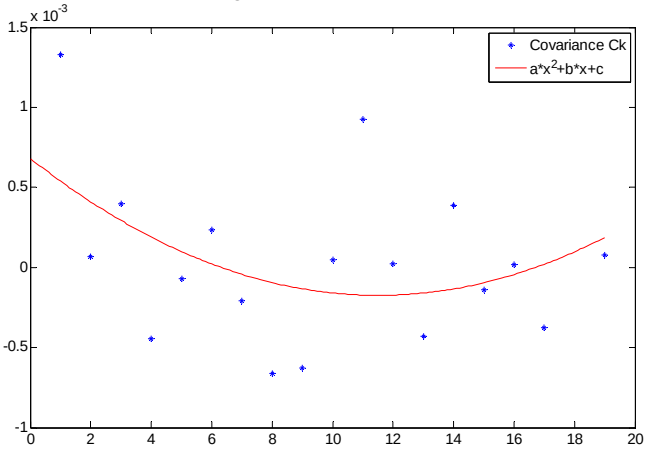

Figure 4: Calculated covariances C_k per counter k for boresight misalignment angle ω and the fitted curve C(r).

Next the design matrix **A** is created according to the mathematical model between the boresight misalignment components and the positions of buildings. After some tests a third-degree surface (Equation [18]) was chosen as the most suitable model.

$$z = a_1 + a_2x + a_3x^2 + a_4x^3 + a_5y + a_6xy + a_7yx^2 + a_8y^2 + a_9y^2x + a_{10}y^3 \quad (18)$$

Based on the surface in Equation [18] and Equations [8], [9] and [10], the best values $\hat{\mathbf{x}}$ of parameters in Equation [18] are defined. From Equations [14] and [15] the a posteriori variation of unit weight $\hat{\sigma}_o^2$ and the a posteriori covariance matrix $\hat{\mathbf{V}}_{\hat{x}}$ of $\hat{\mathbf{x}}$ are calculated. As a criterion of the overall success of the fitting, the comparison of the ratio $\hat{\sigma}_o^2/\sigma_o^2$ by χ^2 distribution is used. In addition, as a criterion of meaningfulness of the surface's coefficients, the ratio $a_i/\hat{\sigma}_o$ is compared to the corresponding value of t distribution. The need for using all of the ten factors a_1, a_2, ..., a_{10} was evidenced. Figure 5 illustrates the fitted surface for boresight angle ω. Note that angle φ has a similar fitted surface with angle ω, while κ angle is different.

In order to find the minimum density of known buildings the procedure of simulations are performed. Positions are multiplied by scale factors and the procedure of fitting is repeated. In particular for the new positions, the covariance values C_k and the parameters a, b and c of curve C(r) are calculated by Equa-

tion [7]. Through Equations [8], [9] and [10] the parameters of surface of Equation [18] are calculated, while from Equations [14] and [15] the corresponding criteria of precision are calculated.

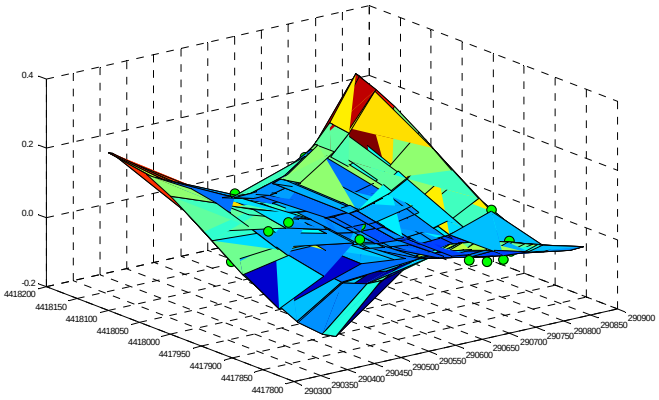

Figure 5: Fitted surface to the values of boresight angle ω per building (green circles).

Next the previous procedure is repeated for known positions, the distances of which are growing according to an increasing scale until the number of C_k is stabilized.

As a criterion of the buildings' density, the smaller of the covariance function solutions C(r) is used. This solution is assumed to correspond to the maximum distance of which the known positions should be located in order to have a zero correlation. This distance corresponds to the limit beyond which the interpolation to determine the boresight values will be affected only by the success of the fitting of surface (Equation [18]) and not by the information of the variation of the corresponding boresight misalignment value transferred via signal $\mathbf{s_1}$.

In the whole range of scale factor, for all three angles, the fitting by Equation [18] was particularly satisfactory as demonstrated by the ratio $\hat{\sigma}_o^2/\sigma_o^2$.

For assessing the ability of the fitted surface on the angles' values, each angle in different positions of the field is calculated. 'Buildings-positions' separated by distance as determined according to the previous paragraph, are included in this field.

This determination is made by Equations [16], [17] and [18], using vector $\hat{\mathbf{x}}$ of best values $\hat{a}_i$ of surface in Equation [18], as provided by Equations [9] and [10]. Matrices $\mathbf{V}_{\mathbf{s},\mathbf{s}_1}$ and $\mathbf{V}_{\mathbf{s}_1,\mathbf{s}_1}$ are calculated by C(r), using r as the distance which separates the positions of the available measurements and the positions of the estimates. The positions of the estimates comprised the common center of gravity of all buildings as well as both positions inside and outside of the perimeter formed by the outmost buildings. The application showed that the estimated values, of the three angles with their uncertainties, do not show specific changes.

7. CONCLUSIONS

Under operational circumstances, the values of the boresight misalignment are never accurately known and could only be estimated. Furthermore, boresight misalignment parameters could change over a relatively short time period.

Therefore, having a mechanism to almost continuously check the validity of the boresight misalignment is a valuable tool. In other words, the detection of possible changes in the values in the boresight misalignment through a QA/QC validation process, can assure a sustained product's quality.

In Pothou *et al.,* 2008, a procedure for performing an efficient and fast tool for estimating parameters and detecting any changes in real time or post-processing mode has been proposed. The feasibility of using urban areas for boresight misalignment has been also investigated. Moreover, the influence of the number and distribution of the necessary 'building-positions' on boresight's misalignment parameter estimation has been also evaluated.

In this research, the impact of the spatial distribution and distance between the necessary 'building-positions' on the boresight's misalignment parameter estimation is evaluated by collocation method. Knowledge of the maximum distance that could separate 'buildings positions' is crucial for optimal flight planning because it directly affects the cost of the project.

The minimum density of the 'building-positions' in LiDAR and photogrammetry datasets for boresight misalignment estimation is in the range of 8-10km, for typical airborne surveying conditions. However, this distance depends on the choice of the appropriate covariance function C(r). The selection of function C(r) is based on the successful fitting of the C_k which, in turn, depends, to some degree, on the choice of step d.

The future research objective is the evaluation of the whole process for a larger dataset, including more buildings and covering a greater area. Also, the more detailed investigation on the selection of the covariance function could be analyzed.

8. REFERENCES

Baltsavias, E.P., 1999. Airborne laser scanning: basic relations and formulas. *ISPRS Journal of Photogrammetry & Remote Sensing* 54, pp. 199-214.

Burman, H., 2000. Adjustment of Laser Scanner Data for Correction of Orientation Errors. *IAPRS*, Vol. XXXIII, Part B3, pp. 125-132.

Burman, H., 2002. Laser strip adjustmenr for data calibration and verification. *ISPRS Journal of Photogrammetry & Remote Sensing*, Com. VI, Symposium, part A, WG VI/4, Graz, Austria.

Cross, P., 1990. "Advanced Least Squares Applied to Position – Fixing". *Polytechnic of East London,* Working Paper No.6, p.p. 142-158.

Csanyi, N., 2008. A rigorous approach to comprehensive performance analysis of state-of-the-art airborne mobile mapping systems. *Department of Civil and Environmental Engineering and Geodetic Science, The Ohio State University,* Phd.

Habib, A., Bang, K.I., Shin S., Mitishita E., 2007. LiDAR system self-calibration using planar patches from photogrammetric data. *MMT'07, 'The 5th International Symposium on Mobile Mapping Technology'*, Padua, Italy.

Kremer, J., 2006. System Calibration of aerial camera/GPS/IMU systems - Procedure and experiences. *International Calibration and Orientation Workshop, EUROCOW,* Castelldefels, pp. 6.

Mikhail, E., 1976. Observations and Least Squares. *IEP Series in Civil Engineering, Dun-Donnelley Publisher,* New York.

Morin, K., and El-Sheimy, N., 2002. Post-mission adjustment of airborne laser scanning data. *Proceedings XXII FIG International Congress*, Washington DC, USA, CD ROM.

Moritz, H., 1989. Advanced Physical Geodesy. *Herbert Wichmann Verlag 2nd ed., Karlsruhe*.

Pothou A., Karamitsos S., Georgopoulos A., and Kotsis I., 2006. Assessment and comparison of registration algorithms between aerial images and laser point clouds. *ISPRS, Symposium:'From sensor to imagery',* Com. 1, WGI/2, Part A, France.

Pothou A., Toth C., Karamitsos S., and Georgopoulos A., 2007. On using QA/QC techniques for LiDAR/IMU boresight misalignment. *MMT'07, 'The 5th International Symposium on Mobile Mapping Technology'*, Padua, Italy.

Pothou A., Toth C., Karamitsos S., and Georgopoulos A., 2008. An approach to optimize reference ground control requirements for estimating LiDAR/IMU boresight misalignment. *XXI Congress ISPRS*, WG-I/2, China.

Schenk, T., Krupnik A., and Postolov Y., 2000. Registration of airborne laser data to surfaces generated by Photogrammetric means. *IAPRS*, 32(3/W14), pp. 95-99.

Schenk, T., 2001. Modeling and Analyzing Systematic Errors in Airborne Laser Scanners. *Technical Notes in Photogrammetry, The Ohio State University,* Vol. 19, Columbus, USA.

Shan, J., and Toth, Ch., 2008. Topographic Laser Ranging and Scanning: Principles and Processing, *Published by CRC Press*.

Skaloud, J., and Lichti D., 2006. Rigorous approach to bore-sight self-calibration in airborne laser scanning. *ISPRS, Journal of Photogrammetry & Remote Sensing, Vol.* 61, pp. 47-59.

Skaloud, J., and Schaer, P., 2007. Towards automated LiDAR Boresight self-calibration. *MMT'07, 'The 5th International Symposium on Mobile Mapping Technology',* Padua, Italy.

Toth, C., and Csanyi, N., 2001. Automating the LiDAR Bore-sight Misalignment. *ISPRS, Workshop on 3-D Mapping from InSAR and LiDAR*, WGII/2, Banff, Canada, CD ROM.

Toth, C., 2002. Calibrating Airborne LiDAR Systems, ISPRS Commission II Symposium on Integrated Systems for Spatial Data Production. Custodian and Decision Support, *IAPRS*, Vol. XXXIV, part 2, pp. 475-480.